Received: 4 August 2023 | Revised: 10 July 2024 | Accepted: 23 August 2024

DOI: 10.1111/bph.17348

RESEARCH ARTICLE

Tetrabenazine, a vesicular monoamine transporter 2 inhibitor, inhibits vesicular storage capacity and release of monoamine transmitters in mouse brain tissue

Pál Tod[1] | Anita Varga[2] | Viktor Román[2] | Balázs Lendvai[2] | Roland Pálkovács[2] | Beáta Sperlágh[1] | E. Sylvester Vizi[1,3]

[1]Laboratory of Molecular Pharmacology, HUN-REN Institute of Experimental Medicine, Budapest, Hungary

[2]Pharmacology and Drug Safety Research, Gedeon Richter Plc, Budapest, Hungary

[3]Department of Pharmacology and Pharmacotherapy, Semmelweis University, Budapest, Hungary

Correspondence
E. Sylvester Vizi, Laboratory of Molecular Pharmacology, Institute of Experimental Medicine, Hungarian Research Network, Szigony u. 43, 1083 Budapest, Hungary.
Email: ves@koki.hu

Funding information
Recovery and Resilience Facility of the European Union within the framework of Programme Széchenyi Plan Plus, Grant/Award Number: RRF-2.3.1-21-2022-00011

Abstract

Background and Purpose: Tetrabenazine (TBZ), used for treating hyperkinetic disorders, inhibits vesicular monoamine transporter-2 (VMAT-2), which sequesters monoamines into vesicles for exocytosis. However, our knowledge of the effect of TBZ on monoaminergic transmission is limited. Herein, we provide neurochemical evidence regarding the effect of VMAT-2 inhibition on vesicular neurotransmitter release from the prefrontal cortex (PFC) and striatum (STR) (brain regions involved in characteristic TBZ treatment side effects). The interaction between TBZ and MDMA was also assessed regarding motor behaviour in mice.

Experimental Approach: Vesicular storage capacity and release of [^{3}H]-noradrenaline ([^{3}H]-NA), [^{3}H]-dopamine ([^{3}H]-DA), [^{3}H]-serotonin ([^{3}H]-5-HT), and [^{3}H]-acetylcholine ([^{3}H]-ACh) was studied in mouse PFC and STR ex vivo slice preparations using electrical field stimulation. Additionally, locomotor activity was assessed in vehicle-treated mice and compared with that of MDMA, TBZ, and co-administered animals (n = 6) using the LABORAS system.

Key Results: TBZ lowered the storage capacity and inhibited the vesicular release of [^{3}H]-NA and [^{3}H]-DA from the PFC, and [^{3}H]-DA and [^{3}H]-5-HT from the STR in a concentration-dependent manner. Unlike vesamicol (vesicular ACh uptake inhibitor), TBZ failed to inhibit the vesicular release of [^{3}H]-ACh from the PFC. When the vesicular storage of the investigated monoamines was inhibited by TBZ in the PFC and STR, MDMA induced the release of transmitters through transporter reversal; MDMA dose dependently increased locomotor activity in vivo.

Conclusion and Implications: Our observations provide neurochemical evidence explaining the mechanism of VMAT-2 inhibitors in the brain and support the involvement of dopaminergic and noradrenergic transmission in hyperkinetic movement disorders.

Abbreviations: HPβCD, (2-hydroxypropyl)-beta-cyclodextrin; β-PEA, β-phenylethylamine; PFC, prefrontal cortex; STR, striatum; TBZ, Tetrabenazine.

KEYWORDS
acetylcholine, exocytosis, hyperkinesis, mouse model, tetrabenazine, vesicular monoamine transport proteins

1 | INTRODUCTION

Selective blockade of the **vesicular monoamine transporter 2** protein (VMAT-2) by **tetrabenazine** (TBZ), deutetrabenazine, and valbenazine effectively treats hyperkinetic movement disorders in various populations (Jankovic, 1982; J. J. Chen et al., 2012; Caroff et al., 2018). These disorders are classified as "rare" diseases, and the pharmacological agents developed for their treatment are considered orphan drugs. TBZ has been approved by the United States (US) Food and Drug Administration specifically for the clinical management of chorea symptoms (Margolis, 2014) associated with Huntington's disease (Ricciardi et al., 2019); it is also used off-label for treating tardive dyskinesia (Caroff et al., 2018). VMAT-2 is exclusively responsible for the sequestration of cytoplasmic monoamine transmitters, such as **noradrenaline** (NA), **dopamine** (DA), and **serotonin** (5-hydroxytryptamine, 5-HT), into vesicles (Erickson & Varoqui, 2000; Henry et al., 1994). Nevertheless, there are limited data on the effects of VMAT-2 inhibitors on noradrenergic, dopaminergic, and serotoninergic transmission (Meyer et al., 2011; Volz et al., 2006; Wang et al., 2010). This is particularly relevant in the context of the effect on the vesicular and quantal release of NA and DA in the noradrenergic and dopaminergic nerve terminals in the prefrontal cortex (PFC) and striatum (STR), respectively, as well as serotoninergic neurotransmission in the STR (Mathur & Lovinger, 2012; Wang et al., 2010). These two regions of the brain play critical roles in depression (Koenigs & Grafman, 2009) and parkinsonism, which are side effects observed in clinical studies of VMAT-2 inhibitors (Caroff et al., 2018; Margolis, 2014).

The PFC is a unique location for studying noradrenergic transmission as it exhibits dense noradrenergic innervation (Schwarz & Luo, 2015) originating from the locus coeruleus. Furthermore, in this region, the expression of the **noradrenaline transporter** (NET) is considerably higher than that of the **dopamine transporter** (DAT) (Moll et al., 2000); this area also receives sparse dopaminergic input from the ventral tegmental area (Gallo et al., 2022). The STR is rich in dopaminergic innervation due to the nigrostriatal pathway (Rice & Cragg, 2008) and has moderate serotoninergic (Steinbusch, 1981) and poor noradrenergic innervation (Fitoussi et al., 2013). Furthermore, a growing body of evidence shows that monoamines can be taken up by different types of monoamine transporters (e.g., DAT and NET) at least to a certain extent. Indeed, NA can be taken up and released by **serotonin transporter**s (SERT) (Vizi et al., 2004), and NET is capable of DA uptake in the PFC (Morón et al., 2002). This promiscuity may be related to the shared structural homology of the transporters (Di Chiara et al., 1992).

Vesicular acetylcholine transporters (**VAChT**s) and VMAT-2 are members of the SLC18 family of vesicular transporters. VAChT shares 40% amino acid identity with VMAT-2 (Anne & Gasnier, 2014) and is responsible for transporting **acetylcholine** (ACh) from the cytosol into vesicles for action potential-dependent exocytosis (Sudhof, 2012).

Although the biochemical mechanism of VMAT-2 inhibition by TBZ is established (Nickell et al., 2014), there is a lack of information regarding how TBZ affects the storage capacity and vesicular release of monoamines (e.g., NA, DA, and 5-HT) and ACh. Hence, to gain further insights into the mechanism of TBZ on neuronal transmission and signalling, we utilized mouse ex vivo brain slice preparations and systematically examined the influence of TBZ on the vesicular storage capacity and release of [^{3}H]-NA- and [^{3}H]-DA related radioactivity from the PFC, and [^{3}H]-DA and [^{3}H]-5-HT from the STR tissue slices. Additionally, we sought to link the in vitro effects with **MDMA**-induced hyperlocomotion in mice and elucidate the

What is already known

- The VMAT-2 inhibitor tetrabenazine effectively treats hyperkinetic disorders.
- VMAT-2 inhibitors elicit side effects, including depression and parkinsonism.

What does this study add

- Tetrabenazine does not affect plasma membrane transporter activity but inhibits storage capacity and vesicular release.
- MDMA induces cytoplasmic release of monoamines and hypermotility when vesicular release is inhibited by tetrabenazine.

What is the clinical significance

- Our findings imply that unopposed superactive dopaminergic and noradrenergic innervations contribute to hyperkinesis disorders.
- Tetrabenazine does not prevent MDMA-induced hypermotility, accounting for low efficacy in treating psychostimulant addiction.

mechanisms underlying the efficacy of VMAT-2 inhibitors in the treatment of various hyperkinetic movement disorders, including tardive dyskinesia.

2 | METHODS

2.1 | Animals

In this study, 318 WT male Crl:CD1(ICR) (RRID:IMSR_CRL:022) mice (aged 5–8 weeks, 25–33 g) were used for ex vivo experiments. Only male mice were used to eliminate the potential effects of the oestrous cycle on animal behaviour. WT mice were bred and genotyped at the Medical Gene Technology Unit of the Institute of Experimental Medicine (43 Szigony Str Budapest 1083, Hungary). Animals were maintained on a 12:12 light/dark cycle (lights on 07:00) in a temperature- (23 ± 2°C) and humidity-controlled room (60 ± 10%), with access to food (ssniff® Souris-Elevage E, 10 mm pellet, Cat# S8189-S096; ssniff Spezialdiäten GmbH, Soest, Germany) and water ad libitum. In total, six adult littermates per cage were housed in standard mouse cages with corncob bedding. Cardboard bedding materials and tubes were placed in all cages for environmental enrichment. For in vivo experiments, 99 WT male (Naval Medical Research Institute, Crl:NMRI [Han] [RRID:IMSR_CRL:605]) mice (aged 3 weeks, 18–20 g) were purchased from Toxi-Coop Ltd. (Budapest, Hungary). Animals were housed in groups of four for 7 days before behavioural testing in standard mouse cages with wood chip bedding under a 12:12 light/dark cycle (lights on 06:00) in a controlled environment at a constant temperature (22 ± 2°C) and humidity (55 ± 5%); the animals had access to food and water ad libitum.

The ex vivo experimental protocol was approved by the Semmelweis University Regional Committee (No. 116/2015) and the Institutional Committee of Science and Research Ethics (PE) EA/285-5/2020. The in vivo study protocol was approved by the Richter Plc. Institutional Ethical Committee (PE/EA/648-7/2021).

All experimental procedures strictly followed the guidelines of the European Community Council Directive (2010/63/EU) and the recommendations of the Committee on Animals in Research (FENS). The animals were treated in accordance with ethical guidelines; all efforts were made to minimize animal suffering and reduce the number of experimental animals. Sample size was estimated using G*Power 3.1.9.7 software (RRID:SCR_013726) (Faul et al., 2009): *t* test; a priori: compute required sample size; power: 0.7; α error probability: 0.05; effect size (d): 1.367; total sample size: 12; [^{3}H]-NA release after first stimulation (FRS1, see later) between control versus 3-μM tetrabenazine groups. In total, 387 animals were used in these studies.

Animal studies were performed in accordance with the ARRIVE guidelines 2.0 (Percie du Sert et al., 2020), and with the recommendations made by the *British Journal of Pharmacology* (Lilley et al., 2020). The numbers of mice in each experimental group are shown in the corresponding figure legends. The mice were randomly assigned to experimental groups, and the investigators were blinded to the experimental status of the mice.

2.2 | Materials

The following chemicals were used for the release experiments: levo-[7-^{3}H]-norepinephrine (specific activity = 20 Ci mmol^{-1}), 3,4-[7,8-^{3}H(N)]-dihydroxyphenylethylamine (specific activity = 20 Ci mmol^{-1}), 5-hydroxytryptamine (specific activity = 80 Ci mmol^{-1}), and (^{3}H)-choline chloride (specific activity = 80 Ci mmol^{-1}). All radioactively labelled chemicals were purchased from American Radiolabelled Chemicals, Inc. (Saint Louis, MO, US). Additionally, (2-hydroxypropyl)-beta-cyclodextrin (HPβCD) was purchased from Roquette (Lestrem, France). The VMAT-2 inhibitor TBZ (IUPAC name: 9,10-dimethoxy-3-(2-methylpropyl)-1,3,4,6,7,11b-hexahydrobenzo [a]quinolizin-2-one, Cat# 2175), sodium channel blocker tetrodotoxin citrate (IUPAC name: (1R,5R,6R,7R,9S,11S,12S,13S,14S)-3-amino-14-(hydroxymethyl)-8,10-dioxa-2,4-diazatetracyclo[7.3.1.17,11.01,6]tetradec-3-ene-5,9,12,13,14-pentol, Cat# 1069), and MDMA hydrochloride (IUPAC name: 1-(1,3-benzodioxol-5-yl)-N-methylpropan-2-amine; hydrochloride, Cat# 3027) for in vivo experiments were purchased from Tocris Bioscience (Minneapolis, MN, US). The NET blocker **nisoxetine** hydrochloride (IUPAC name: 3-(2-methoxyphenoxy)-N-methyl-3-phenylpropan-1-amine, Cat# N151), dopamine transporter (DAT) blocker **GBR 12909** dihydrochloride (IUPAC name: 1-[2-[bis(4-fluorophenyl)methoxy]ethyl]-4-(3-phenylpropyl)piperazine, Cat# D052), vesicular ACh inhibitor (±)-**vesamicol** hydrochloride (IUPAC name: 2-(4-phenylpiperidin-1-yl)cyclohexan-1-ol, Cat# V100), trichloroacetic acid (Cat# T0669), hemicholinium-3 (Cat# H108), and dimethyl sulfoxide (Cat# 276855) were obtained from Sigma-Aldrich (St. Louis, MO, US). The MDMA (IUPAC name: 1-(1,3-benzodioxol-5-yl)-N-methylpropan-2-amine;hydrochloride, Cat# 64057-70-1) used for ex vivo experiments was purchased from the National Measurement Institute of the Australian Government (Canberra, Australia). Isoflurane was purchased from Medicus Partner Ltd. (Isofluran CP 1 ml·ml^{-1}, 250 ml, Cat# 1214, CP-Pharma Handelsgesellschaft mbH, Germany).

2.3 | Release of [^{3}H]-NA, [^{3}H]-DA, and [^{3}H]-5-HT from prefrontal cortex (PFC) and striatum (STR) slices

Mice were killed in a two-step manner according to the American Veterinary Medical Association guidelines for the Euthanasia of Animals: 2020 Edition (available online: https://www.avma.org/sites/default/files/2020-02/Guidelines-on-Euthanasia-2020.pdf). First, the animals were anaesthetised with a high dose of isoflurane (>1.5 v/v %) in a sufficiently large container to ensure rapid loss of consciousness and prevent hypoxia. The mice were then decapitated, and the brain was immediately removed and placed into ice-cold Krebs solution (composition in mM: 113 NaCl, 4.7 KCl, 1.2 $MgSO_4$, 2.5 $CaCl_2$, 25 $NaHCO_3$, 1.2 KH_2PO_4, 115 glucose, 0.3 Na_2EDTA, and 0.03 ascorbic acid), which was continuously saturated with carbogen (mixture of 95% O_2 and 5% CO_2). For the experiments performed in calcium-free conditions, 1-mM EGTA was added, and the slice preparations were incubated in the modified Krebs solution throughout the experimental period.

The PFC and STR were isolated, and then 400-μm thick slices were cut using a tissue chopper. The viability of most cells in thin hippocampal and neocortical brain slices is limited to 6–12 h, and a healthy state can only be maintained for approximately 4 h (Buskila et al., 2014). Hence, the slice preparations were used within a maximum of 2.5 h to maintain the neuroanatomical structure and function. Furthermore, under normal conditions, monoamine transporters located in the plasma membrane can take up monoamines (e.g., NA, DA, and 5-HT) from the extracellular space in humans and animals, albeit to varying extents (Han & Gu, 2006). Accordingly, in our setup, we replicated the clinical treatment with selective serotonin reuptake inhibitors (SSRIs).

The slices were incubated with [^{3}H]-NA, [^{3}H]-DA, or [^{3}H]-5-HT up to a concentration of 3 μCi in 1-ml Krebs solution for 45 min. To investigate the effects of TBZ, the drug was added to the Krebs perfusate and incubated until the end of the measurement. Subsequently, the preparations were washed three times with 10 ml of ice-cold, oxygenated Krebs solution and transferred to a two-channel microvolume (100 μl) perfusion apparatus (Vizi et al., 1985) maintained at 37°C. Four slices were used in each chamber, and the preparation was superfused with Krebs solution at a rate of 0.5 ml·min^{-1} for 60 min before each measurement. A low perfusion rate (0.5 ml·min^{-1}) was applied as the superfusion speed is expected to influence the uptake by removing transmitters released into the fluid (Raiteri et al., 1974). These procedures were performed at similar settings compared with earlier studies (Baranyi et al., 2006; Lakatos et al., 2020) in which the amount of tritiated [^{3}H]-NA or [^{3}H]-DA transmitters and the presence of their metabolites were detected through high-pressure liquid chromatography combined with radiochemical detection. Accordingly, the release of radioactivity measured in slice preparations, either under resting conditions or in response to stimulation, was considered representative of the loaded tritiated transmitters and transmitter-derived metabolites.

After preperfusion, nineteen 3-min fractions were sampled during the release experiments. The supramaximal level of electrical field stimulation (Grass S88 stimulator, parameters: PFC: [^{3}H]-NA: 20 V, 2 Hz, 2 ms, and 2 min; [^{3}H]-DA: 20 V, 2 Hz, 2 ms, and 3 min; STR: [^{3}H]-NA and [^{3}H]-DA: 40 V, 2 Hz, 1 ms, and 1 min; [^{3}H]-5-HT: 40 V, 2 Hz, 2 ms, and 1 min) was applied to the third (S1) and 13th fractions (S2). In the MDMA study on [^{3}H]-NA release in the presence or absence of nisoxetine (NIS) after tetrabenazine pretreatment, only S1 was applied to the third fraction (20 V, 2 Hz, 2 ms, and 1 min), and S2 was omitted. Nisoxetine (10 μM) was added to the sixth fraction, and MDMA (30 μM) was added to the eighth fraction; both drugs were allowed to remain until the end of the experiment. To examine the effects of MDMA and β-PEA on the resting release of neurotransmitters, no stimulation was applied. To clarify whether the release of [^{3}H]-NA and [^{3}H]-DA from the PFC or STR, respectively, was dependent on electrical stimulus and Ca^{2+}, we applied 1-μM tetrodotoxin (TTX), 10-μM TBZ, and TBZ + nisoxetine (1 μM or 10 μM) from the eighth collection period until the end of the experiments. Furthermore, Ca^{2+}-free conditions were established from the sixth collection period using 1-mM EGTA.

The supernatant (500 μl) from each fraction was added to 2 ml of scintillation mixture (Ultima Gold; Packard, Canberra, Australia). After sample collection, the tissues were extracted from the chambers, and the remaining radioactively labelled neurotransmitters were extracted with 5 ml of 10% trichloroacetic acid for 30 min; 100 μl of the supernatant was added to 2 ml of scintillation mixture, and the radioactivity was measured using a Packard 1900 Tricarb and 5110 TR liquid scintillation counter (Packard). The radioactivity values were expressed as disintegrations per minute per gram of wet tissue (Becquerels per gram, Bq·g^{-1}).

The uptake of [^{3}H]-NA, [^{3}H]-DA, and [^{3}H]-5-HT by the tissue slices was defined as the radioactivity content of the tissue at the start of the perfusion period (C_B). This value was estimated using Equation (1):

$$\sum_i 1 - 19\,FR_i + C_E = C_B \quad (1)$$

where FR_i is the radioactivity in fraction number i and C_E is the remaining tissue radioactivity content measured at the end of the experiment.

The electrical field stimulation (S1 and S2)-induced release was calculated based on the total release of radioactivity over the resting release (R1 and R2, respectively). R1 was considered the average radioactivity release in the first and second fractions, and R2 was the average release of radioactivity in the 14th and 15th fractions.

2.4 | Vesicular storage capacity and cytoplasmic content of [^{3}H]-NA, [^{3}H]-DA, and [^{3}H]-5-HT

The uptake of [^{3}H]-NA, [^{3}H]-DA, and [^{3}H]-5-HT into the tissue slices was measured in control conditions and at a range of TBZ concentrations (PFC: [^{3}H]-NA: 0.3–30 μM, [^{3}H]-DA: 1–30 μM; STR: [^{3}H]-DA: 0.03–10 μM, [^{3}H]-5-HT:1–10 μM) and (10 μM GBR 12909) (DAT blocker). In brief, 10–12 tissue slices were incubated for 45 min in a 1-mL organ bath containing Krebs solution continuously oxygenated and maintained at 37°C. During this period, 3 μl of [^{3}H]-NA, 5 μl of [^{3}H]-DA, and 5 μl of [^{3}H]-5-HT were added to the solution. Then, the slices were washed three times, and the radioactively labelled neurotransmitters were extracted with 5 ml of 10% trichloroacetic acid for 30 min. A 100-μl aliquot of the supernatant was added to 2 ml of scintillation mixture (Ultima Gold; Packard); the radioactivity was measured using a Packard 1900 Tricarb and 5110 TR liquid scintillation counter (Packard) and expressed in terms of disintegrations per minute per gram of wet tissue (Bq·g^{-1}).

In experiments in which the supramaximal concentration of TBZ was added with radioactively labelled transmitters during the loading period, the electric field stimulation-evoked release of radioactivity was inhibited, indicating that the vesicles were empty. Therefore, the radioactive content of the tissue measured under this condition was defined as the cytoplasmic content of the terminal. The difference from the content measured in tissues taken from control animals indicated the percentage of terminal vesicular content.

2.5 | Release of [^{3}H]-ACh from prefrontal cortex (PFC) slice preparations

PFC slices were prepared as previously described for the experiments designed for measuring the release of monoamines. First, a 45-min incubation with [^{3}H]-choline (5 μCi·ml^{-1}) was carried out in a 1-ml organ bath containing Krebs solution maintained at 37°C. To examine the effects of TBZ or vesamicol, the drugs were added to the solution and remained throughout the experimental period. At the end of the incubation period, the slices were transferred to the microvolume perfusion system and washed five times with Krebs solution. Four slices were placed in each chamber and superfused with Krebs solution at a rate of 0.5 ml·min^{-1} for 60 min. To prevent the reuptake of [^{3}H]-choline—a byproduct of the degradation of released [^{3}H]-ACh following hydrolysis—the superfusing Krebs solution contained 10 μM hemicholine-3 (Vizi et al., 1984). After 60 min of preperfusion, the effluent was discarded. Next, 19 3-min samples were collected, and the tissues were stimulated twice at the third fraction (Stim 1) and 13th fraction (Stim 2). Supramaximal electrical train stimulation was performed using a Grass S88 stimulator with the following parameters: 20 V, 2 Hz, 2 ms, and 2 min.

ACh is synthesized in the cytoplasm, and vesicles are loaded with ACh by the VAChT. Electric field stimulation primarily increases the release of [^{3}H]-ACh from the vesicles but not that of [^{3}H]-choline from the nerve terminals (Vizi et al., 1987). Accordingly, under conditions in which choline reuptake is prevented by hemicholine, the increase in radioactivity measured in the perfusion fluid in response to stimulation is due to the labelled choline degraded from the released [^{3}H]-ACh. Supernatant (500 μl) from each fraction was added to 2 ml of scintillation mixture (Ultima Gold; Packard). After sample collection, the tissues were removed, and the residual [^{3}H]-ACh was extracted using 5 ml of 10% trichloroacetic acid for 30 min. Subsequently, 100 μl of supernatant was added to 2 ml of scintillation mixture; the radioactivity was determined using a liquid scintillation counter (Packard 1900 Tricarb and 5110 TR) and reported as disintegration per minute per gram of wet tissue (Bq·g^{-1}).

2.6 | Fractional release calculations

The radioactivity in the samples was shown as fractional release (FR) using the following customized formula (Equation 2):

$$FR\% = \frac{\textit{released tritium in Bq/g} \times 100}{\textit{tritium in Bq/g in the tissue at the time of sample measurement}} \quad (2)$$

The exocytotic release of [^{3}H]-NA or [^{3}H]-DA was determined by integrating the amount of release over the baseline in response to supramaximal electrical field stimulation (at the 13th [S_2] and third fractions [S_1]) in the presence (FRS_2) and absence (FRS_1) of the drug; the FRS_2/FRS_1 ratio was then calculated to show the effects of the drug studied. The release produced by S_1 was considered the internal standard. Similarly, the effect on the resting release was measured using the FRR_2/FRR_1 ratio, where FRR_1 was used as the internal standard based on the average radioactivity collected during the first and second periods, if not otherwise indicated.

2.7 | Behavioural assessment of tetrabenazine (TBZ)- and MDMA-treated mice

The effects of MDMA and TBZ on locomotor activity were assessed in WT male NMRI mice (aged 4 weeks, 24–31 g). Mice were transferred to the study room 1 day prior to the experiment for acclimatization. On the experiment day, the mice were treated with MDMA (5, 10, or 15 mg·kg^{-1}, i.p., dissolved in physiological saline) and TBZ (4 mg·kg^{-1}, i.p., dissolved in 5% DMSO and 23.75% HPβCD in 0.01-M PBS). Control animals were administered the corresponding vehicle. The two treatments were directly administered one after the other to the opposite sides of the animals. Locomotor activity was monitored between 8:00–14:00 h using a system designed for the detection of various form of movements (LABORAS™, Metris B.V., Hoofddorp, The Netherlands; monitors the general behaviour in mice). The LABORAS consists of a triangular platform made of sensing carbon fibres (700 × 700 × 1000 × 30 mm) on two orthogonal force transducers and a third fixed leg on a bottom plate (Corian Plate 695 × 695 × 980 × 48 mm). The system is located on three external vibration-absorbing spikes. The mechanical vibrations generated by the movement of the animals were recorded along with the movement trajectory. Locomotor effects were assessed for up to 60 min starting immediately after TBZ and/or MDMA administration.

2.8 | Data and statistical analysis

The data and statistical analysis comply with the recommendations for experimental design and analysis in pharmacology (Curtis et al., 2022). We calculated the number of animals required per group using G*Power 3.1.9.7 software. Values in the paper were expressed as the mean ± SEM (error bars), or geometric mean ± 95% confidence index (CI), where the date was analysed after $\log_{10}$ transformation. For in vitro experiments n = 6 animals, for in vivo experiments n = 9 animals, were used per group. The declared group size is the number of independent values; the statistical analysis was performed using these independent values. The normality of the data distribution was assessed using the Shapiro–Wilk test. In the case of a non-normal distribution or when Bartlett's test indicated heterogeneity of variances, a $\log_{10}$ transformation was performed. If Bartlett's test still indicated heterogeneity of variances, the Kruskal–Wallis one-way ANOVA by rank followed by Dunn's test or Welch's ANOVA were used. To estimate the significant difference of the control group to other groups, one-way ANOVA followed by Dunnett's

post hoc test was conducted. For between-group comparisons, one-way ANOVA followed by Tukey's post hoc test or two-way ANOVA with Dunnett's post hoc test with or without repeated measures were used. Post-hoc tests were run only if F achieved P<0.05 and there was no significant variance inhomogeneity. Post hoc tests were considered statistically significant if $P < 0.05$. To compare two groups, a two-tailed unpaired *t* test or, in the case of non-normally distributed data, a two-tailed Mann–Whitney U-test was used; these tests were considered statistically significant if $P < 0.05$. Fold changes were calculated compared with the mean control value or lowest dose and expressed as mean ± SEM. IC_{50} values were calculated using R package dr4pl to calculate a 4-parameter logistic model with 95 confidence intervals on default. Meaning that sum of squares was calculated and Nelder–Mead optimisation was used. Statistical analyses and data visualization were conducted using GraphPad Prism 8 (GraphPad Software Inc., San Diego, CA, USA; RRID:SCR_002798).

2.9 | Nomenclature of targets and ligands

Key protein targets and ligands in this article are hyperlinked to corresponding entries in http://www.guidetopharmacology.org, and are permanently archived in the Concise Guide to PHARMACOLOGY 2021/22 (Alexander Christopoulos et al., 2023; Alexander Fabbro et al., 2023).

3 | RESULTS

3.1 | Effects of tetrabenazine (TBZ) on resting and stimulation-evoked release of transmitters from the prefrontal cortex (PFC) and striatum (STR) in ex vivo slice preparations

The removal of Ca^{2+} from the superfusate or application of the Na^+ channel inhibitor tetrodotoxin following the first (S1) stimulation inhibited the S2-evoked release of radioactivity from PFC slices loaded with [^{3}H]-NA (Table 1). This indicates that the transmitter release in response to stimulation was action-potential-dependent and vesicular in origin. TBZ significantly promoted the release under resting conditions, even in a Ca^{2+}-free environment, but failed to elevate the release through electrical stimulation, similar to plasma transporter inhibitors (Table 1). Indeed, nisoxetine, a selective NET inhibitor known to block transportation in both directions, potentiated the S2-evoked [^{3}H]-NA release and prevented TBZ from increasing the resting release (Table 1).

To further analyse the electrical field stimulation-evoked release in ex vivo slice preparations, the exocytotic release of [^{3}H]-DA was examined in the STR. Ca^{2+}-free conditions and tetrodotoxin application (starting from the sixth fraction) prevented the stimulation-evoked release of radioactivity (Table 2). These results (Tables 1 and 2) provide convincing evidence that the release of labelled

TABLE 1 Effects of tetrabenazine on $[Ca^{2+}]_o$-independent resting and $[Ca^{2+}]$–dependent vesicular release of [^{3}H]-noradrenaline from mouse prefrontal cortex (PFC) tissue. PFC slices were incubated with tetrodotoxin (1 μM), tetrabenazine (10 μM), and nisoxetine (1 μM or 10 μM) from the eighth collection period until the end of the experiment. Ca^{2+}-free conditions were established from the sixth collection period, and 1-mM EGTA was added to the Krebs solution (incubation medium). Electrical field stimulation (2 Hz, 120 shocks) was evoked at the third and 13th fractions. The resting release ratio (FRR_2/FRR_1) and the stimulation release (FRS_2/FRS_1) ratio were expressed as FR%. One-way ANOVA (between treatments: $F[6, 35] = 30.29$, $P < 0.05$) followed by Tukey's multiple comparisons post hoc test (FRR_2/FRR_1), Welch's ANOVA test (between treatments: $W[6, 15.38] = 169.4$, $P < 0.05$) followed by Holm–Sidak multiple comparisons post hoc test (FRS_2/FRS_1): $^*P < 0.05$ compared with the control group; $^+P < 0.05$ compared with tetrabenazine no Ca^{2+} + 1-mM EGTA group; $^\$P < 0.05$ compared with tetrabenazine + nisoxetine 10 μM group; $^aP < 0.05$ compared with tetrabenazine 10 μM group; $^bP < 0.05$ compared with nisoxetine 1 μM group.

Treatment	FRR_2/FRR_1	FRS_2/FRS_1
Control	0.92 ± 0.03	0.86 ± 0.03
Tetrodotoxin 1 μM	0.85 ± 0.02$^+$	0.12 ± 0.02$^{*,\$,a,b}$
No Ca^{2+} + 1-mM EGTA	0.87 ± 0.03$^+$	0.11 ± 0.02$^{*,\$,a,b}$
Tetrabenazine no Ca^{2+} + 1-mM EGTA	1.41 ± 0.05*	0.16 ± 0.03^{*,b}
Tetrabenazine + nisoxetine 10 μM	0.99 ± 0.04$^+$	1.33 ± 0.10$^{*,+}$
Tetrabenazine 10 μM	1.61 ± 0.09$^{*,+,\$}$	0.64 ± 0.07$^{+,\$}$
Nisoxetine 1 μM	0.82 ± 0.04$^+$	1.34 ± 0.04$^{*,+,a}$

Note: Values are expressed as mean ± SEM (n = 6 mice per group).
Abbreviations: [^{3}H], tritium; FRR, resting release ratio; FRS, stimulation released ratio; PFC, prefrontal cortex.

TABLE 2 $[Ca^{2+}]_o$-independent resting and $[Ca^{2+}]$-dependent vesicular release of [^{3}H]-dopamine from mouse striatal slice preparations. Striatal slices were exposed to tetrodotoxin (1 μM), and Ca^{2+}-free conditions (0.03-mM 1-mM EGTA was added to the Krebs solution [incubation medium]) were established from the sixth collection period and maintained throughout the experiment. Electrical field stimulation (2 Hz, 120 shocks) was evoked at the third and 13th (in case of Ca^{2+}-free condition at the 15th) fractions. The resting release ratio (FRR_2/FRR_1) and the stimulation release (FRS_2/FRS_1) ratio are expressed as FR%. Values are expressed as mean ± SEM (n = 6 mice per group). Kruskal–Wallis test (FRR_2/FRR_1): $P = 0.0639$ and one-way ANOVA (between treatments: $F[2, 15] = 191.2$, $P < 0.05$) followed by Tukey's multiple comparisons post hoc test (FRS_2/FRS_1): $^*P < 0.05$ compared with control group; $+P < 0.05$ compared with tetrodotoxin 1 μM group.

Treatment	FRR_2/FRR_1	FRS_2/FRS_1
Control	0.64 ± 0.01	0.70 ± 0.02
Tetrodotoxin 1 μM	0.5 ± 0.02	0.09 ± 0.04*
No Ca^{2+} + 1-mM EGTA	0.57 ± 0.07	−0.04 ± 0.02$^{*,+}$

Note: Values are expressed as mean ± SEM.
Abbreviations: [^{3}H], tritium; FRR, resting release ratio; FRS, stimulation released ratio.

transmitters in response to electrical stimulation, calculated at the top of the release at rest (see Methods), is of vesicular origin and can be attributed to exocytosis.

3.2 | Effects of tetrabenazine (TBZ) on vesicular storage capacity in prefrontal cortex (PFC) and striatum (STR) slices

To determine the vesicular storage capacity of the tissue preparations, [^{3}H]-NA and [^{3}H]-DA were loaded with different concentrations of TBZ into the PFC slices. In the case of [^{3}H]-NA, the administration of TBZ at concentrations of 0.3, 3, 10, and 30 μM resulted in a significant decrease in tissue radioactivity content compared with the control group, representing a reduction in tissue vesicular storage capacity (Figure 1a). The calculated IC_{50} value was 0.24 μM (lower 95% CI: 0.17, upper 95% CI: 0.3). Moreover, no significant alterations were observed between the effect of TBZ administered at 10 and 30 μM, indicating that the vesicles were empty and that the remaining ~10% resided in the cytoplasm; ~90% of the radioactively labelled neurotransmitters were stored in vesicles in the noradrenergic terminals. Similarly, the inhibition of [^{3}H]-DA vesicular storage capacity by TBZ in the PFC slices at 1, 3, 10, and 30 μM led to a significant decrease compared with the control group (Figure 1b). The calculated IC_{50} value for TBZ was 1.84 μM (lower 95% CI: -17.95, upper 95% CI: 21.63).

As the STR is abundantly innervated by dopaminergic neurons, the effect of TBZ on the radioactive content in this tissue was studied further. TBZ was loaded at 0.03- 10 μM in conjunction with [^{3}H]-DA and 1-10-μM TBZ and 10-μM GBR 12909, a competitive inhibitor of dopamine uptake, with [^{3}H]-5-HT into STR slices. Compared with the control group, TBZ induced an 18.28%, 42.94%, 37.14%, 64.97%, and 88.68% decrease in [^{3}H]-DA content at 0.03, 0.1, 0.3, 1, and 10 μM, respectively (Figure 1c). The calculated IC_{50} value for TBZ for this activity was 0.03 μM (lower 95% CI: 0.02, upper 95% CI: 0.04). Compared with the control group, TBZ induced a 14.64%, 38.87%, and 77.82% reduction in [^{3}H]-5-HT content at 1, 3, and 10 μM, respectively. The tissue radioactivity content was markedly reduced after 3- and 10-μM TBZ application compared with the control group (Figure 1d). The calculated TBZ IC_{50} value for this activity was 2.46 μM (lower 95% CI: 2.46, upper 95% CI: 2.5). Furthermore, 10-μM GBR 12909 administration did not altered the [^{3}H]-5-HT uptake into STR slices and showed a significant difference compared with the groups treated with 3- and 10-μM TBZ.

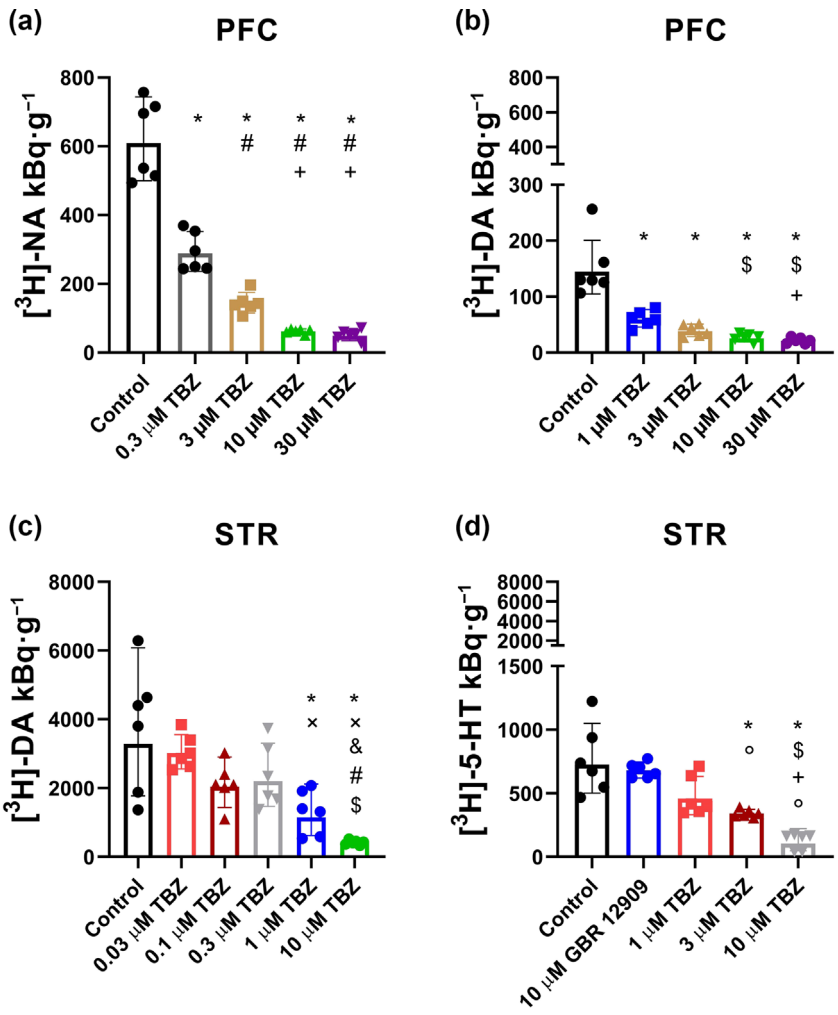

FIGURE 1 Effects of tetrabenazine (TBZ) on the vesicular storage capacity of [^{3}H]-noradrenaline ([^{3}H]-NA), [^{3}H]-dopamine ([^{3}H]-DA), and [^{3}H]-5-hydroxytryptamine ([^{3}H]-5-HT) in the mouse prefrontal cortex (PFC) and striatum (STR). The brain tissue slices were incubated with various TBZ concentrations (PFC: [^{3}H]-NA: 0.3, 3, 10, and 30 μM; [^{3}H]-DA: 1, 3, 10, and 30 μM; and STR: [^{3}H]-DA: 0.03, 0.1, 0.3, 1, and 10 μM; [^{3}H]-5-HT: 1, 3, and 10 μM). (a) Effect of TBZ on the vesicular storage capacity of [^{3}H]-NA in the PFC. (b) Effect of TBZ on the vesicular storage capacity of [^{3}H]-DA in the PFC. (c) Effect of TBZ on the vesicular storage capacity of [^{3}H]-DA in the STR. (d) Effect of TBZ on the vesicular storage capacity of [^{3}H]-5-HT in the STR. Values are expressed as geometric mean ± 95% CI with n = 6 mice per group. One-way ANOVA with log transformation (between groups: (a): $F[4; 25] = 140$, $P < 0.05$; (b): $F[4, 25] = 46.51$, $P < 0.05$; (c): $F[5, 30] = 21.57$, $P < 0.05$; (d): $F[4, 25] = 24.45$, $P < 0.05$) followed by Tukey's multiple comparisons post hoc test: $^*P < 0.05$ compared with control group; $^\times P < 0.05$ compared with 0.03-μM TBZ group; $^\&P < 0.05$ compared with 0.1-μM TBZ group; $^\#P < 0.05$ compared with 0.3-μM TBZ group; $^\$P < 0.05$ compared with 1-μM TBZ group; $^+P < 0.05$ compared with 3-μM TBZ group; $^\circ P < 0.05$ compared with GBR 12909 group. Abbreviations: [^{3}H], tritium; NA, noradrenaline; DA, dopamine; TBZ, tetrabenazine; PFC, prefrontal cortex; STR, striatum.

3.3 | Effect of VMAT-2 inhibition by tetrabenazine (TBZ) on the stimulation-evoked vesicular release of radioactivity from prefrontal cortex (PFC) and striatum (STR) slice preparations loaded with [^{3}H]-NA, [^{3}H]-DA, or [^{3}H]-5-HT

We studied the stimulation-evoked vesicular release of radioactivity from slice preparations loaded with [^{3}H]-NA and [^{3}H]-DA in the presence of 3-, 10-, and 30-μM TBZ; 10- and 30-μM TBZ application inhibited the Stim1- and Stim2-induced release of [^{3}H]-NA from the PFC, revealing that the stimulation-evoked release was similarly reduced as the vesicular storage capacity was reduced in a concentration-dependent manner (Figure 2a). Similarly, the stimulation-evoked release of [^{3}H]-DA was inhibited by TBZ at all applied doses in the PFC compared with the control group at S1 and S2 (Figure 2b).

The modulatory actions of TBZ on [^{3}H]-DA and [^{3}H]-5-HT release were also studied in STR slice preparations (Figure 3a,b). Results show that 1-μM TBZ significantly decreased the electric field stimulation-evoked release of [^{3}H]-DA from STR compared with the control group. In the case of [^{3}H]-5-HT (Figure 3b), 10-μM TBZ markedly decreased the electric field stimulation-evoked release of [^{3}H]-5-HT from STR compared with the control group. Compared with the control group, although 3-μM TBZ application did not significantly alter the electric field stimulation-evoked release of [^{3}H]-5-HT from STR, a marked difference was observed between the groups treated with 1 and 3 μM in comparison to 10-μM TBZ group.

3.4 | Effects of tetrabenazine (TBZ) on [^{3}H]-ACh release from prefrontal cortex (PFC) slices

While VMAT-2 is responsible for replenishing vesicles with monoamines, VAChT is responsible for the vesicular uptake of ACh. In this study, vesamicol inhibited the electric field stimulation-evoked release

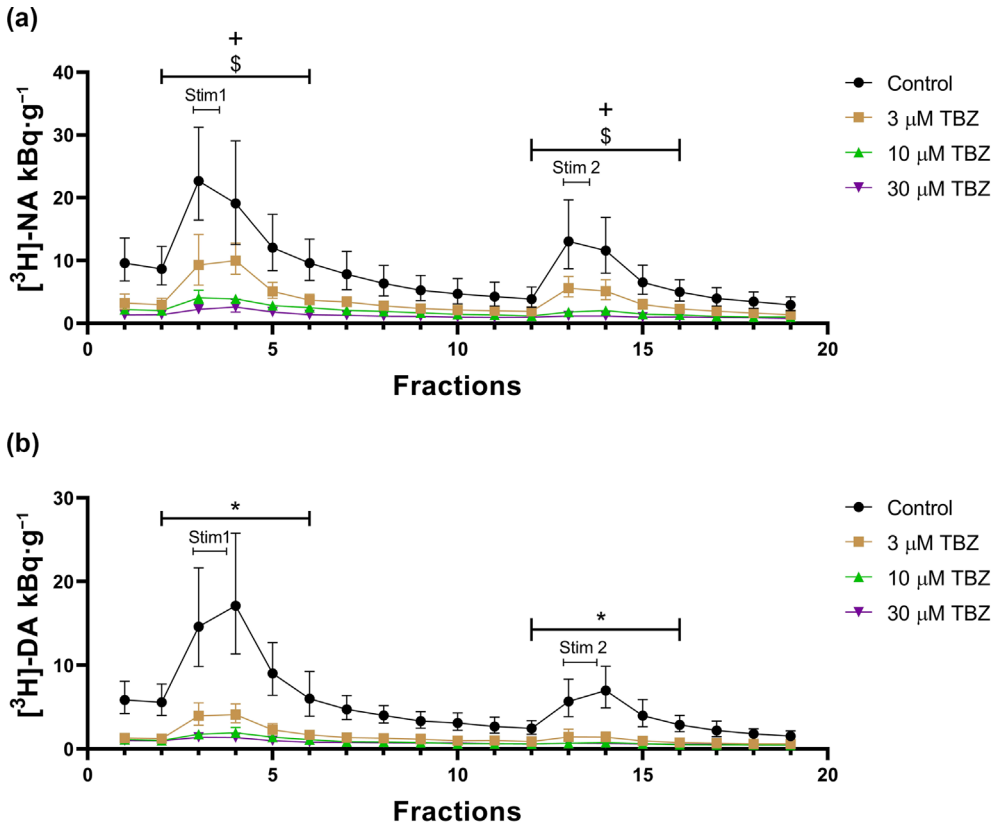

FIGURE 2 Effects of tetrabenazine (TBZ) on the release of [^{3}H]-noradrenaline ([^{3}H]-NA) and [^{3}H]-dopamine ([^{3}H]-DA) in the mouse prefrontal cortex (PFC). Tissue slices were incubated in Krebs solution; TBZ (3, 10, and 30 μM) was introduced during the incubation and was allowed to remain until the end of the experiment. The tissue slices were stimulated at the third (Stim 1) and 13th (Stim 2) fractions ([^{3}H]-NA: 20 V, 2 Hz, 2 ms, and 2 min; [^{3}H]-DA: 20 V, 2 Hz, 2 ms, and 3 min). The released radioactivity was measured in the collected fractions. (a) The efflux of [^{3}H]-NA was markedly decreased in the presence of 10- and 30-μM TBZ and (b) in case of [^{3}H]-DA at all doses at S1 and S2 compared with that in the control group. Values are expressed as geometric mean ± 95% CI with n = 6 mice per group. One-way ANOVA with log transformation (compared with control group: (a): S1: $F[3, 20] = 31.21$, $P < 0.05$, S2: $F[3, 20] = 36.46$, $P < 0.05$; (b): S1: $F[3, 20] = 94.57$, $P < 0.05$, S2: $F[3, 18] = 31.41$, $P < 0.05$) followed by Dunnett's multiple comparisons post hoc test: $^*P < 0.05$ compared with control group; $^+P < 0.05$ compared with 10-μM TBZ group; $^\$P < 0.05$ compared with 30-μM TBZ group. Abbreviations: [^{3}H], tritium; NA, noradrenaline; DA, dopamine; TBZ, tetrabenazine; PFC, prefrontal cortex; S1, first electric field stimulation; S2, second electric field stimulation.

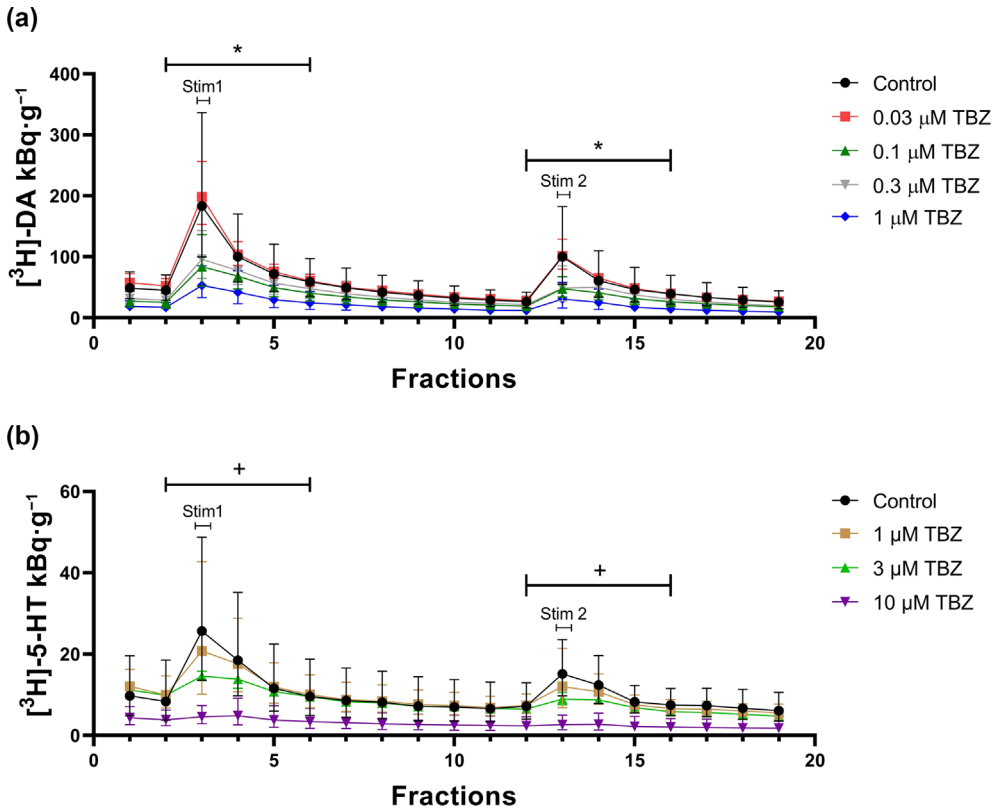

FIGURE 3 Effect of tetrabenazine (TBZ) on [^{3}H]-dopamine ([^{3}H]-DA) and [^{3}H]-5-hydroxytryptamine ([^{3}H]-5-HT) release in the mouse striatum (STR). Tissue slices were incubated in Krebs solution; TBZ ([^{3}H]-DA: 0.03, 0.1, 0.3, and 1 μM; [^{3}H]-5-HT: 1, 3, and 10 μM) was introduced during the incubation and allowed to remain until the end of the experiment. The tissue slices were stimulated at the third (Stim 1) and 13th (Stim 2) fractions ([^{3}H]-DA: 40 V, 2 Hz, 1 ms, and 1 min; [^{3}H]-5-HT: 40 V, 2 Hz, 2 ms, and 1 min). The released radioactivity was measured in the collected fractions. (a) [^{3}H]-DA release was markedly decreased in the presence of TBZ throughout the experimental period compared with that in the control group. (b) [^{3}H]-5-HT release was significantly decreased after 10-μM TBZ application upon electric field stimulation (S1 and S2) and at fractions four to eight and 14 to nine compared with the control group. Values are expressed as geometric mean ± 95% CI with n = 6 mice per group. One-way ANOVA with log transformation ((a): S1: $F[4, 25] = 6.358$, $P < 0.05$, S2: $F[4, 25] = 5.64$, $P < 0.05$; (b): $F[3, 20] = 14.87$, $P < 0.05$, S2: $F[3, 20] = 17.26$, $P < 0.05$) followed by (a) Dunnett's and (b) Tukey's multiple comparisons post hoc test: $^*P < 0.05$ compared with 1-μM TBZ, $^+P < 0.05$ compared with 10-μM TBZ. Abbreviations: [^{3}H], tritium; DA, dopamine; TBZ, tetrabenazine; STR, striatum; S1, first electric field stimulation; S2, second electric field stimulation.

of [^{3}H]-ACh from PFC compared with the control and TBZ administered groups at S1. TBZ did not affect the electric field stimulation-evoked release of [^{3}H]-ACh (Figure 4a). Neither vesamicol nor TBZ affected [^{3}H]-ACh uptake into the tissue slices (Figure 4b).

3.5 | Effect of plasma membrane monoamine transporter substrates on the release of radioactive cytoplasmic NA and DA from the prefrontal cortex (PFC) and striatum (STR)

As neurochemical evidence of the proportional distribution of radioactivity between vesicular and cytoplasmic contents (~90% vs. ~10%; see Figure 1) was obtained, we sought to evaluate the effects of MDMA and β-phenylethylamine (β-PEA)—known to release NA and DA from the cytoplasm by transporter reversal (Zsilla et al., 2018)—on the transmitter outflow from the cytoplasm when the vesicular replenishment of NA or DA was partially or fully inhibited by TBZ. To examine this aspect, animals were pre-treated with TBZ (4 mg·kg^{-1}) to ensure that no new vesicles could be loaded with [^{3}H]-NA (in the case of the PFC) or [^{3}H]-DA (in the case of the STR). No marked difference was observed in response to the electrical field stimulation (S1) at the third fraction. In the PFC, MDMA, introduced from the eighth fraction, significantly increased [^{3}H]-NA efflux from the PFC from fraction 10 compared with that when the reuptake of [^{3}H]-NA was inhibited by nisoxetine (added from the sixth fraction). In the presence of NIS, MDMA failed to release radioactivity, indicating the role of transporter reversal and the cytoplasmic origin (Figure 5a). Next, the resting release of [^{3}H]-DA was measured from STR slice preparations loaded with 10-μM TBZ. We found that 10-μM β-PEA or 30-μM MDMA, added to the tissue at the eighth fraction, significantly elevated the resting release. Meanwhile, if the DAT inhibitor GBR 12909 was applied at the sixth fraction, the elevating effect of MDMA was counteracted (Figure 5b).

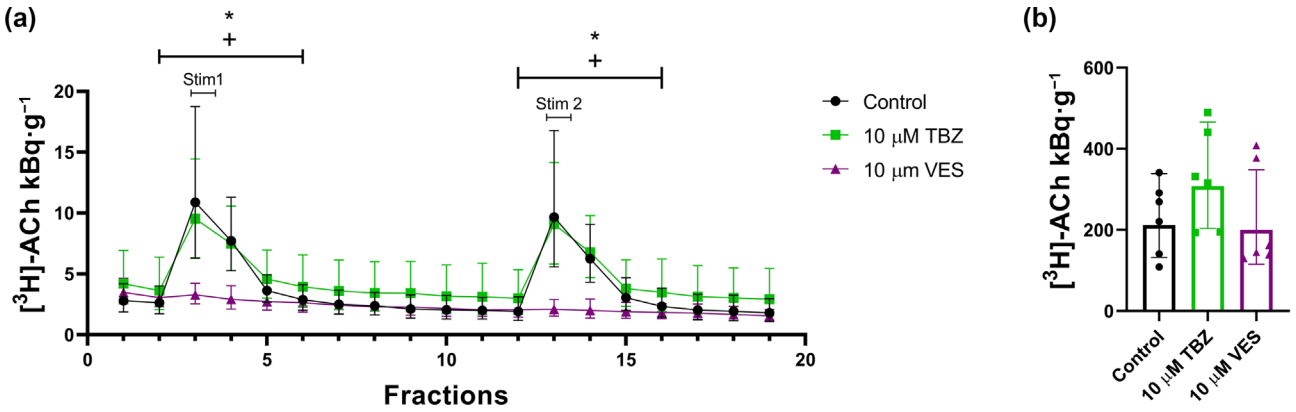

FIGURE 4 Effect of vesamicol (VES) and tetrabenazine (TBZ) on [^{3}H]-acetylcholine ([^{3}H]-ACh) release and uptake in the mouse prefrontal cortex (PFC). Tissue slices were incubated in Krebs solution; TBZ (10 μM) or vesamicol (10 μM) was added during the incubation and allowed to remain until the end of the experiment. The tissue slices were stimulated at the third (Stim 1) and 13th (Stim 2) fractions (20 V, 2 Hz, 2 ms, and 2 min). The released radioactivity was measured in the collected fractions. (a) Compared with that in the control and TBZ groups, [^{3}H]-ACh release in response to electric field stimulations (S1 and S2) was lower in the vesamicol group. TBZ did not alter [^{3}H]-ACh release upon S1 and S2 stimulation. (b) [^{3}H]-ACh uptake into tissue. Neither 10-μM TBZ nor 10-μM vesamicol altered [^{3}H]-ACh uptake in the tissue slices. Values are expressed as geometric mean ± 95% CI with n = 6 mice per group. One-way ANOVA with log transformation ((a): S1: $F[2, 15] = 75.89$, $P < 0.05$, S2: $F[2, 14] = 73.7$, $P < 0.05$; (b): $F[2, 15] = 1.55$, $P = 0.244$) followed by Tukey's multiple comparisons post hoc test: $^*P < 0.05$ compared with control group; $^+P < 0.05$ compared with TBZ group. Abbreviations: [^{3}H], tritium; ACh, acetylcholine; TBZ, tetrabenazine; VES, vesamicol; PFC, prefrontal cortex; S1, first electric field stimulation; S2, second electric field stimulation.

3.6 | Effects of tetrabenazine (TBZ) on mouse locomotor activity and MDMA-induced hypermotility

To investigate the effect of TBZ on hyperkinesia, hyperlocomotion was induced by MDMA treatment in mice. MDMA treatment caused a marked increase in the locomotion time at 5 and 15 mg·kg^{-1} doses compared with that in the control group (Figure 6a). In contrast, 4 mg·kg^{-1} TBZ treatment significantly reduced locomotor activity (Figure 6b). To test the hypothesis that TBZ treatment could prevent MDMA-induced hyperactivity, mice were co-administered MDMA (5, 10, 15 mg·kg^{-1}) and TBZ (4 mg·kg^{-1}). TBZ significantly inhibited the elevation in locomotor activity induced by 5 mg·kg^{-1} MDMA. TBZ reduced hyperlocomotion even in animals treated with 10 and 15 mg·kg^{-1} MDMA, although this reduction was not complete and not significant (Figure 6c).

4 | DISCUSSION

It is widely accepted that the quantal exocytotic release of transmitter-containing vesicles is dependent on $[Ca^{2+}]_o$, action potential-evoked Na^+ influx, and the activity of VMAT-2 at the axonal terminal, which transports transmitters into vesicles (John & Jones, 2006). Sustained neuronal activity, followed by appropriate exocytosis, requires rapid replenishment of storage vesicles with NA, DA, or 5-HT. Unlike reserpine, which blocks VMAT-2 and VMAT-1 (Carlsson, 1966), resulting in depression and hypotension (Darchen et al., 1989; Metzger et al., 2002), TBZ is a selective inhibitor of VMAT-2, the predominant isoform in the brain that is exclusively responsible for resupplying vesicles that reside in the cytosol with NA, DA, or 5-HT. Although the biochemical effects of TBZ and its derivations on VMAT-2 are well described (Nickell et al., 2014), minimal data are available on how neurochemical signalling is affected in the PFC and STR, two brain regions involved in the pathomechanism of depression and parkinsonism.

To study the role of VMAT-2 inhibition in transmitter release, we identified two distinct release types: (i) external Ca^{2+}- and tetrodotoxin-sensitive release induced by electrical stimulation, corresponding to release from synaptic vesicles and (ii) $[Ca^{2+}]_o$-independent release at rest in the absence of electrical stimulation, corresponding to direct release from the cytoplasm. The acute application of TBZ in this system could induce an increase in resting release while failing to influence vesicular release. This is likely due to the increase in cytoplasmic transmitter content, which is the driving force underlying release at rest in vitro in preloaded slices. In this study, the long-term application of TBZ (when loaded with tritiated transmitters) left sufficient time to empty the synaptic vesicles. Consequently, we observed reduced storage capacity of the synaptic vesicles in the slices, as measured by their radioactivity content. However, the IC_{50} values showed that the inhibitory effect of TBZ on monoamine storage capacity and electric field stimulation were similar for NA and DA, and lower for 5-HT. We showed for the first time that the inhibition of VMAT-2 with TBZ reduced the storage capacity of monoaminergic axon terminals in a concentration-dependent manner. Additionally, when VMAT-2 was inhibited, electric field stimulation failed to evoke the vesicular release of [^{3}H]-NA, [^{3}H]-DA, and [^{3}H]-5-HT from the PFC and STR slices. Accordingly, when the release was measured from terminals pretreated with TBZ, the stimulation-evoked vesicular release markedly decreased, as evidence by the S1 values. However, unlike vesamicol, TBZ did not reduce the vesicular release

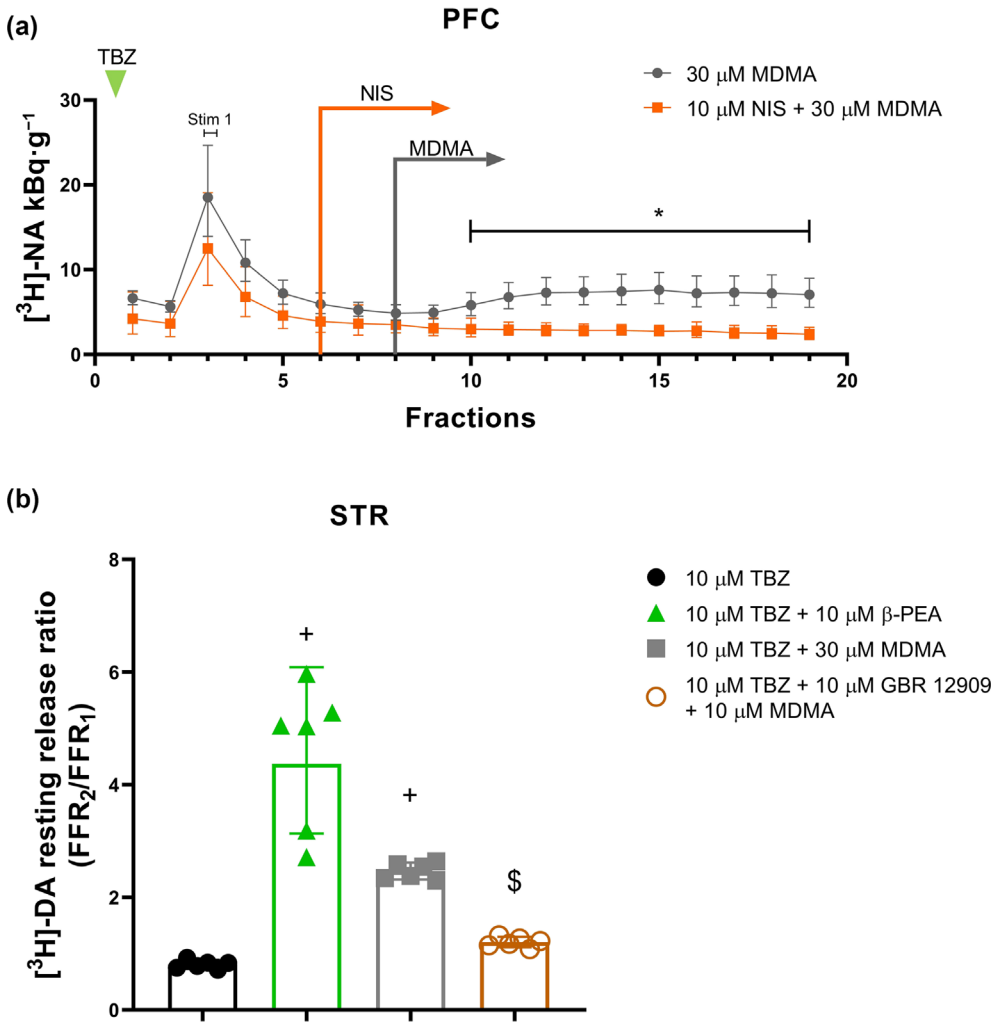

FIGURE 5 Effect of MDMA and β-PEA, substrates of the monoamine transporters, on cytoplasmic [^{3}H]-noradrenaline ([^{3}H]-NA) and [^{3}H]-dopamine ([^{3}H]-DA) release from mouse prefrontal cortex (PFC) and striatum (STR) slice preparations. Animals were pre-treated with 4 mg·kg^{-1} tetrabenazine (TBZ) and killed after 60 min (for PFC), or the STR tissue samples were incubated with 10-μM TBZ. Brain tissue slices were prepared and stimulated at the third (S1) fraction ([^{3}H]-NA: 20 V, 2 Hz, 2 ms, and 2 min; [^{3}H]-DA: 40 V, 2 Hz, 1 ms, and 1 min) in the case of the PFC or no stimulus was applied (STR). (a) Upon electric field stimulation, the release of both [^{3}H]-NA (in fraction 3) markedly differed between the study groups. Nisoxetine (NIS) was introduced at the sixth fraction, and MDMA was added at the eighth fraction. After the release of the vesicles loaded with [^{3}H]-NA in PFC in response to electrical field stimulation, MDMA was still able to induce [^{3}H]-NA efflux if the noradrenaline transporter (NET) was not inhibited from the 12th fraction (a). (b) Resting release (resting release ratio [FRR2/FRR1; fifth, sixth vs. 12th, 13th fractions]) of [^{3}H]-DA was markedly elevated by MDMA and β-PEA (applied at the eighth fraction). The dopamine transporter (DAT) inhibitor GBR 12909 (applied at the sixth fraction) inhibited the [^{3}H]-DA efflux in response to MDMA. Values are expressed as geometric mean ± 95% CI with n = 6 mice per group. (a) Unpaired *t* test (S1: $t = 1.997$, $df = 10$, $P = 0.0738$) and (b) Kruskal–Wallis test ($F[4, 24] = 21.6$, $P < 0.05$) followed by (a) Sidak and (b) Dunn's multiple comparisons post hoc test: $^*P < 0.05$ compared with 30-μM MDMA group; $^+P < 0.05$ compared with 10-μM TBZ group; $^\$P < 0.05$ compared with 10-μM TBZ + 30-μM MDMA group. Abbreviations: [^{3}H], tritium; NA, noradrenaline; DA, dopamine; TBZ, tetrabenazine; NIS, nisoxetine; PFC, prefrontal cortex; STR, striatum; S1, first electric field stimulation; DAT, dopamine transporter; NET, noradrenaline transporter.

of [^{3}H]-ACh from the PFC, further confirming that it is selective for VMAT-2 transporters, although VMAT-2 and VAChT share a 40% sequence identity (Anne & Gasnier, 2014). Regarding the promiscuity of the monoamine transporters, it is important to note that TBZ blocks only the vesicular uptake of monoamines into the axon terminals, without influencing the plasmalemmal uptake. Indeed, while TBZ markedly reduced the vesicular release of both NA and DA from the PFC upon stimulation, nisoxetine failed to decrease NA release, showing that the effect of TBZ is independent of the plasmalemmal transporter. Therefore, the assumed heterologous uptake does not significantly influence the exocytotic release of monoamines. Furthermore, GBR 12909 administration did not influence the uptake of [^{3}H]-5-HT in the STR, indicating that DAT does not play an important role in 5-HT uptake in the STR, at least at the applied concentrations.

These findings, together with the observation that TBZ failed to enhance stimulation-evoked vesicular release, indicate that the

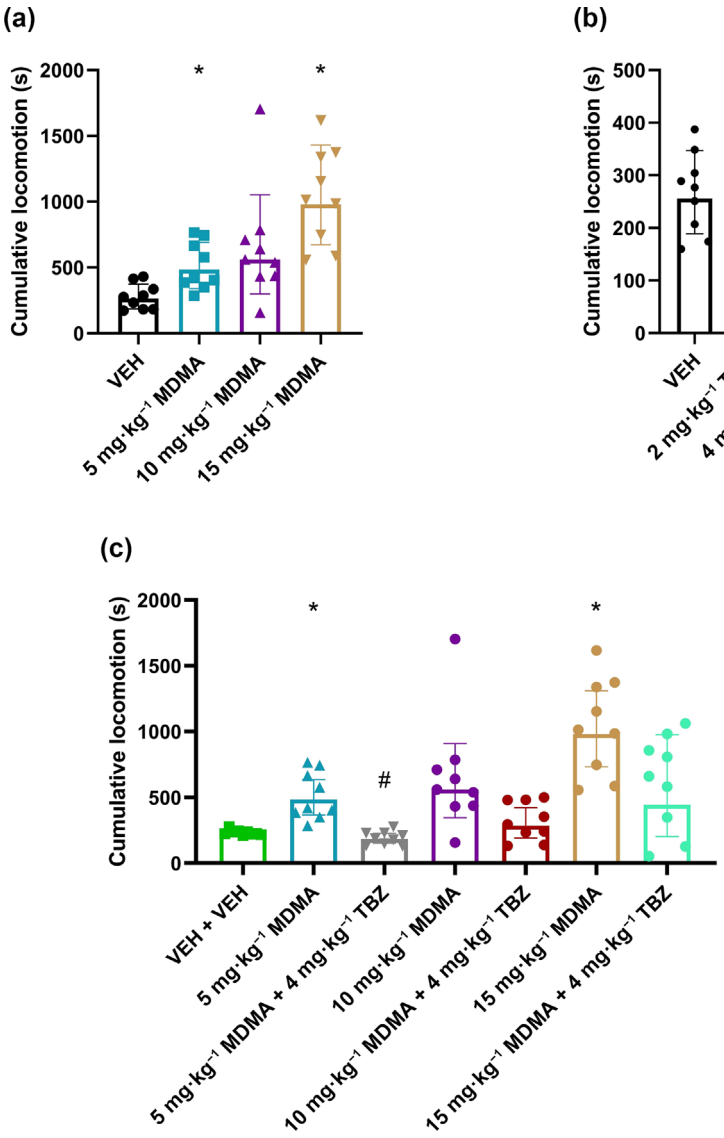

FIGURE 6 Inhibition of MDMA-evoked locomotor activity by tetrabenazine (TBZ) in mice. Mice were treated with MDMA and/or TBZ, and locomotor activity was assessed using the LABORAS system. (a) MDMA caused a marked increase in locomotion time at 5, 10, and 15 mg·kg^{-1} doses at 60 min after drug application. (b) TBZ significantly reduced basic locomotor activity at 4 mg·kg^{-1} doses 60 min after drug application. (c) Co-administration of 4 mg·kg-1 TBZ with 5 mg·kg-1 MDMA reduced the evoked locomotor hyperactivity. Values are expressed as mean ± SEM of n = 9 mice per group. Welch's ANOVA (a): $W = 14.64[3, 15.72]$; $P < 0.05$; (b): $W = 10.49[2, 13.58]$, $P = 0.05$ and (c): $W = 13.5$ $[6, 22.46]$, $P < 0.05$: $^{*}P < 0.05$ compared with VEH group; $^{\#}P < 0.05$ compared with 5 mg·kg^{-1} MDMA + VEH-treated group. Abbreviations: TBZ, tetrabenazine; VEH, vehicle.

vesicular storage capacity of [^{3}H]-NA, [^{3}H]-DA, and [^{3}H]-5-HT in the PFC and STR terminals was decreased. These findings also imply that plasmalemmal uptake of the transmitter from the extracellular space was not reduced. However, this contradicts several studies that report TBZ to be a monoamine uptake inhibitor (Meyer et al., 2011; Ross & Renyi, 1966). Indeed, [^{3}H]-NA and [^{3}H]-DA readily entered the terminals from the extracellular space via NET or DAT during incubation, while nisoxetine and GBR-12909—two selective inhibitors—prevented their uptake.

VMAT-2 inhibitors are used in the treatment of hyperkinetic disorders, such as Huntington's chorea or tardive dyskinesia. Neurochemical evidence obtained from the post-mortem brain tissues of patients with Huntington's chorea showed that NA and DA levels were elevated in the caudate nucleus (Spokes, 1980). In addition, post-mortem samples from TBZ-treated patients had significantly lower levels of monoamines than those from non-treated controls (Pearson & Reynolds, 1988). However, recent findings suggest that DA transmission is increased in the early stages of Huntington's disease, leading to hyperkinetic movements, and decreases in the later phases (J. Y. Chen et al., 2013; Cepeda et al., 2014). In parallel, while DA innervation was decreased in the STR of the affected people, 5-HT increased (Bedard et al., 2011). Our findings that the monoamine storage capacity of vesicles and the amount of axonal activity-related release were reduced by TBZ provide an explanation for the results of these studies and support the view that unopposed hyperactive dopaminergic and noradrenergic innervation contributes to hyperkinetic movement disorders, at least in the early stages.

VMAT-2 antagonists (TBZ, valbenazine) are used to treat tardive dyskinesia, the prevalence of which is 15–20% among patients with schizophrenia treated with second and third-generation antipsychotics (Carbon et al., 2017; de Tommaso et al., 2011). In TBZ clinical studies, doses ranging from 6.25 to 300 mg·day^{-1} were associated with side effects, such as depression, drowsiness/fatigue, and parkinsonism (Caroff et al., 2018). The PFC is dense in noradrenergic projections originating from the locus coeruleus (Schwarz & Luo, 2015) and plays a critical role in depression (Koenigs & Grafman, 2009) along

with serotonin (Hersey et al., 2022). It also contributes to spatial working memory and decision-making (Jentsch et al., 1997; Williams & Goldman-Rakic, 1995). These determinant features of the PFC may help explain the noradrenergic involvement in the side effects observed during treatment with TBZ. A decrease in the vesicular release of DA from the STR might explain TBZ treatment-induced parkinsonism. Furthermore, a recent study found that TBZ-induced side effects can be counteracted by NLX-112 (befiradol)—a selective **5-HT$_{1A}$ receptor** agonist (Jastrzebska-Wiesek et al., 2022)—thus 5-HT$_{1A}$ agonists may prove beneficial in alleviating TBZ-induced side effects.

Further evidence of the role of TBZ in regulating the release of neurotransmitter-containing vesicles was obtained when brain slices (animals previously treated with TBZ or direct addition of TBZ to the tissue) were exposed to MDMA or β-PEA, also monoamine transporter substrates (Robertson et al., 2009; Zsilla et al., 2018). In these slices, the vesicles exhibited limited storage capacity and impaired vesicular release, while the cytosolic transmitter content was maintained or even increased. Indeed, MDMA induced a substantial release of cytoplasmic [^{3}H]-NA from the PFC if NET was not inhibited by nisoxetine. Moreover, the resting release of [^{3}H]-DA was markedly elevated in response to β-PEA and MDMA application, while the DAT inhibitor GBR 12909 markedly decreased this effect of MDMA in STR tissue slices. These observations align with other studies that indicate that MDMA interacts with monoamine transporters (Gorska & Golembiowska, 2015) to elevate resting release. Hence, the release originated from cytoplasm and was likely caused by the activity reversal of the plasma membrane transporter rather than vesicular release. Furthermore, our findings are consistent with the observation that lobeline—a drug that elevates the resting release under $[Ca^{2+}]_o$-independent conditions—can also inhibit VMAT-2 function (Miller et al., 2004; Santha et al., 2000). Moreover, DAT inhibition counteracted the effect of MDMA on [^{3}H]-DA release in resting conditions, suggesting that DAT inhibitors may be beneficial in treating MDMA addiction. This conclusion seems to be supported by recent findings (Li et al., 2021) that the blockade of SERT by cocaine up-regulates the serotoninergic effect on 5-HT$_{1B}$ receptors and may be useful in drug use disorder therapy.

To establish a connection between the actions of TBZ at the transmitter level and its well-described clinical effects, we performed an in vivo locomotion study in which the action of TBZ and the effect of the hyperlocomotion inducer MDMA and its interactions with tetrabenazine were examined. In accordance with the clinical effect, TBZ lowered locomotion in mice, while MDMA elevated locomotion, showing that these drugs regulate locomotion in an opposing manner. This agrees with the idea that monoamines are needed to increase locomotor activity (Chan & Webster, 1971) and that TBZ-induced loss of vesicular (and resting) release can reduce locomotion. TBZ was found to significantly decrease MDMA-induced hyperkinesia in mice, further explaining its clinical efficacy in hyperkinetic disorders. Importantly, TBZ did not completely block locomotor behaviour at the highest tested dose. MDMA induced locomotion at all the tested doses in the presence of high-dose TBZ, suggesting that vesicular release is responsible for only a fraction of the locomotor behaviour. Cytoplasmic release of monoamines occurs when the animal exhibits hyperlocomotion, as revealed by the ability of MDMA to release [^{3}H]-DA of cytoplasmic origin (Roman et al., 2021) and induce locomotor activity. These findings may also explain why TBZ has not been successful in treating amphetamine drug abuse (Meyer et al., 2011) associated with the dopaminergic reward system.

Our earlier studies revealed forms of in vivo behaviour that could be linked to the non-quantal release of transmitters in the brain, including a bridge between analogue DA signalling evoked by MDMA and the passive social behaviour of rats (Roman et al., 2021). In this study, we reveal another type of behaviour, locomotor activity, which has an evident connection to the cytoplasmic, nonquantal release of monoamines under conditions when the vesicular release is impaired by TBZ.

5 | CONCLUSIONS

Our findings show that TBZ does not inhibit the plasma membrane uptake of monoamines but prevents their vesicular uptake. Furthermore, as TBZ reduces the vesicular storage capacity in the axon terminal, it reduces the amount of quantally released monoamines in response to axonal stimulation, leaving cholinergic release unchanged. Our results also show that TBZ administration reduces but does not antagonize MDMA-induced hyperlocomotion in vivo or MDMA-induced release of NA and DA from the cytoplasm. However, it should be noted that these data are solely derived from male mice, and further investigation is required to understand the vesicular uptake and release of monoamines in female mice. Furthermore, we investigated these effects only on the two most prominent brain areas (PFC in depression and STR in hyperkinetic movement disorders). Nevertheless, other brain areas may also play a role in hyperkinetic disorders, warranting further studies.

AUTHOR CONTRIBUTIONS

Conceptualization and Supervision: E. Sylvester Vizi; Methodology: E. Sylvester Vizi and Balázs Lendvai; Data Curation, Formal Analysis, Visualization, Writing–Original Draft Preparation: Pál Tod; Investigation (ex vivo release experiments): Roland Pálkovács; Investigation (animal behaviour experiments): Anita Varga; Writing–Review and Editing: E. Sylvester Vizi, Balázs Lendvai, Beáta Sperlágh, and Viktor Román. All the authors have read and approved the final version of the manuscript.

ACKNOWLEDGEMENTS

This work was supported by grants from the Eötvös Loránd Research Network 090/2022-23 and by the Recovery and Resilience Facility of the European Union within the framework of Programme Széchenyi Plan Plus (grant number RRF-2.3.1-21-2022-00011, National Laboratory of Translational Neuroscience). The authors would like to thank Mrs. Anita Bagó for assistance with the release experiments and Ms. Orsi Gere for technical support and Dr. Levente Kontra from the

HUN-REN IEM Bioinformatics Core Facility for the help with statistical analysis. The authors state that they did not preregister the research with or without an analysis plan in an independent, institutional registry.

CONFLICT OF INTEREST STATEMENT

The authors declare no conflict of interest.

DATA AVAILABILITY STATEMENT

The data that support the findings of this study are available from the corresponding author upon reasonable request. Some data may not be made available due to privacy or ethical restrictions.

DECLARATION OF TRANSPARENCY AND SCIENTIFIC RIGOUR

This Declaration acknowledges that this paper adheres to the principles for transparent reporting and scientific rigour of preclinical research as stated in the *BJP* guidelines for Design and Analysis and Animal Experimentation and as recommended by funding agencies, publishers, and other organizations engaged with supporting research.

ORCID

Pál Tod https://orcid.org/0000-0001-9163-7071
Anita Varga https://orcid.org/0009-0007-2920-2641
Viktor Román https://orcid.org/0000-0002-4849-3591
Balázs Lendvai https://orcid.org/0000-0001-9289-4715
Roland Pálkovács https://orcid.org/0000-0002-3677-6260
Beáta Sperlágh https://orcid.org/0000-0003-0099-591X
E. Sylvester Vizi https://orcid.org/0000-0002-9557-4597

REFERENCES

Alexander, S. P. H., Christopoulos, A., Davenport, A. P., Kelly, E., Mathie, A. A., Peters, J. A., Veale, E. L., Armstrong, J. F., Faccenda, E., Harding, S. D., Davies, J. A., Abbracchio, M. P., Abraham, G., Agoulnik, A., Alexander, W., Al-Hosaini, K., Bäck, M., Baker, J. G., Barnes, N. M., … Ye, R. D. (2023). The Concise Guide to PHARMACOLOGY 2023/24: G protein-coupled receptors. *British Journal of Pharmacology*, *180*, S23–S144. https://doi.org/10.1111/bph.16177

Alexander, S. P. H., Fabbro, D., Kelly, E., Mathie, A. A., Peters, J. A., Veale, E. L., Armstrong, J. F., Faccenda, E., Harding, S. D., Davies, J. A., Amarosi, L., Anderson, C. M. H., Beart, P. M., Broer, S., Dawson, P. A., Gyimesi, G., Hagenbuch, B., Hammond, J. R., Hancox, J. C., … Verri, T. (2023). The Concise Guide to PHARMACOLOGY 2023/24: Transporters. *British Journal of Pharmacology*, *180*, S374–S469. https://doi.org/10.1111/bph.16182

Anne, C., & Gasnier, B. (2014). Vesicular neurotransmitter transporters: Mechanistic aspects. *Current Topics in Membranes*, *73*, 149–174. https://doi.org/10.1016/B978-0-12-800223-0.00003-7

Baranyi, M., Milusheva, E., Vizi, E. S., & Sperlagh, B. (2006). Chromatographic analysis of dopamine metabolism in a Parkinsonian model. *Journal of Chromatography. A*, *1120*(1–2), 13–20. https://doi.org/10.1016/j.chroma.2006.03.018

Bedard, C., Wallman, M. J., Pourcher, E., Gould, P. V., Parent, A., & Parent, M. (2011). Serotonin and dopamine striatal innervation in Parkinson's disease and Huntington's chorea. *Parkinsonism & Related Disorders*, *17*(8), 593–598. https://doi.org/10.1016/j.parkreldis.2011.05.012

Buskila, Y., Breen, P. P., Tapson, J., van Schaik, A., Barton, M., & Morley, J. W. (2014). Extending the viability of acute brain slices. *Scientific Reports*, *4*, 5309. https://doi.org/10.1038/srep05309

Carbon, M., Hsieh, C. H., Kane, J. M., & Correll, C. U. (2017). Tardive dyskinesia prevalence in the period of second-generation antipsychotic use: A meta-analysis. *The Journal of Clinical Psychiatry*, *78*(3), e264–e278. https://doi.org/10.4088/JCP.16r10832

Carlsson, A. (1966). Drugs which block the storage of 5-hydroxytryptamine and related amines. In V. Erspamer (Ed.), *5-Hydroxytryptamine and related Indolealkylamines. Handbook of experimental pharmacology/Handbuch der experimentellen Pharmakologie* (Vol. 19). Springer. https://doi.org/10.1007/978-3-642-85467-5_11

Caroff, S. N., Aggarwal, S., & Yonan, C. (2018). Treatment of tardive dyskinesia with tetrabenazine or valbenazine: A systematic review. *Journal of Comparative Effectiveness Research*, *7*(2), 135–148. https://doi.org/10.2217/cer-2017-0065

Cepeda, C., Murphy, K. P., Parent, M., & Levine, M. S. (2014). The role of dopamine in Huntington's disease. *Progress in Brain Research*, *211*, 235–254. https://doi.org/10.1016/B978-0-444-63425-2.00010-6

Chan, O. L., & Webster, R. A. (1971). Effect of tetrabenazine and alpha-methyl-m-tyrosine on exploratory activity and brain catecholamines in rats. *British Journal of Pharmacology*, *41*(4), 691–699. https://doi.org/10.1111/j.1476-5381.1971.tb07077.x

Chen, J. J., Ondo, W. G., Dashtipour, K., & Swope, D. M. (2012). Tetrabenazine for the treatment of hyperkinetic movement disorders: A review of the literature. *Clinical Therapeutics*, *34*(7), 1487–1504. https://doi.org/10.1016/j.clinthera.2012.06.010

Chen, J. Y., Wang, E. A., Cepeda, C., & Levine, M. S. (2013). Dopamine imbalance in Huntington's disease: A mechanism for the lack of behavioral flexibility. *Frontiers in Neuroscience*, *7*, 114. https://doi.org/10.3389/fnins.2013.00114

Curtis, M. J., Alexander, S. P. H., Cirino, G., George, C. H., Kendall, D. A., Insel, P. A., Izzo, A. A., Ji, Y., Panettieri, R. A., Patel, H. H., Sobey, C. G., Stanford, S. C., Stanley, P., Stefanska, B., Stephens, G. J., Teixeira, M. M., Vergnolle, N., & Ahluwalia, A. (2022). Planning experiments: Updated guidance on experimental design and analysis and their reporting III. *British Journal of Pharmacology*, *179*(15), 3907–3913. Portico. https://doi.org/10.1111/bph.15868

Darchen, F., Scherman, D., & Henry, J. P. (1989). Reserpine binding to chromaffin granules suggests the existence of two conformations of the monoamine transporter. *Biochemistry*, *28*(4), 1692–1697. https://doi.org/10.1021/bi00430a040

de Tommaso, M., Serpino, C., & Sciruicchio, V. (2011). Management of Huntington's disease: Role of tetrabenazine. *Therapeutics and Clinical Risk Management*, *7*, 123–129. https://doi.org/10.2147/TCRM.S17152

Di Chiara, G., Tanda, G. L., Frau, R., & Carboni, E. (1992). Heterologous monoamine reuptake: Lack of transmitter specificity of neuron-specific carriers. *Neurochemistry International*, *20*(Suppl), 231S–235S. Retrieved from https://www.ncbi.nlm.nih.gov/pubmed/1365432

Erickson, J. D., & Varoqui, H. (2000). Molecular analysis of vesicular amine transporter function and targeting to secretory organelles. *The FASEB Journal*, *14*(15), 2450–2458. https://doi.org/10.1096/fj.00-0206rev

Faul, F., Erdfelder, E., Buchner, A., & Lang, A. G. (2009). Statistical power analyses using G*Power 3.1: Tests for correlation and regression analyses. *Behavior Research Methods*, *41*(4), 1149–1160. https://doi.org/10.3758/BRM.41.4.1149

Fitoussi, A., Dellu-Hagedorn, F., & De Deurwaerdere, P. (2013). Monoamines tissue content analysis reveals restricted and site-specific correlations in brain regions involved in cognition. *Neuroscience*, *255*, 233–245. https://doi.org/10.1016/j.neuroscience.2013.09.059

Gallo, F. T., Zanoni Saad, M. B., Silva, A., Morici, J. F., Miranda, M., Anderson, M. C., Weisstaub, N. V., & Bekinschtein, P. (2022). Dopamine modulates adaptive forgetting in medial prefrontal cortex. *The*

Journal of Neuroscience, *42*(34), 6620–6636. https://doi.org/10.1523/JNEUROSCI.0740-21.2022

Gorska, A. M., & Golembiowska, K. (2015). The role of adenosine A1 and A2A receptors in the caffeine effect on MDMA-induced DA and 5-HT release in the mouse striatum. *Neurotoxicity Research*, *27*(3), 229–245. https://doi.org/10.1007/s12640-014-9501-0

Han, D. D., & Gu, H. H. (2006). Comparison of the monoamine transporters from human and mouse in their sensitivities to psychostimulant drugs. *BMC Pharmacology*, *6*, 6. https://doi.org/10.1186/1471-2210-6-6

Henry, J. P., Botton, D., Sagne, C., Isambert, M. F., Desnos, C., Blanchard, V., Raisman-Vozari, R., Krejci, E., Massoulie, J., & Gasnier, B. (1994). Biochemistry and molecular biology of the vesicular monoamine transporter from chromaffin granules. *The Journal of Experimental Biology*, *196*, 251–262. https://doi.org/10.1242/jeb.196.1.251

Hersey, M., Hashemi, P., & Reagan, L. P. (2022). Integrating the monoamine and cytokine hypotheses of depression: Is histamine the missing link? *The European Journal of Neuroscience*, *55*(9–10), 2895–2911. https://doi.org/10.1111/ejn.15392

Jankovic, J. (1982). Treatment of hyperkinetic movement-disorders with tetrabenazine—A double-blind crossover study. *Annals of Neurology*, *11*(1), 41–47. https://doi.org/10.1002/ana.410110108

Jastrzebska-Wiesek, M., Wesolowska, A., Kolaczkowski, M., Varney, M. A., Newman-Tancredi, A., & Depoortere, R. (2022). The selective 5-HT 1A receptor agonist, NLX-112, overcomes tetrabenazine-induced catalepsy and depression-like behavior in the rat. *Behavioural Pharmacology*, *33*(5), 333–341. https://doi.org/10.1097/FBP.0000000000000681

Jentsch, J. D., Tran, A., Le, D., Youngren, K. D., & Roth, R. H. (1997). Subchronic phencyclidine administration reduces mesoprefrontal dopamine utilization and impairs prefrontal cortical-dependent cognition in the rat. *Neuropsychopharmacology*, *17*(2), 92–99. https://doi.org/10.1016/S0893-133X(97)00034-1

John, C. E., & Jones, S. R. (2006). Exocytotic release of dopamine in ventral tegmental area slices from C57BL/6 and dopamine transporter knockout mice. *Neurochemistry International*, *49*(8), 737–745. https://doi.org/10.1016/j.neuint.2006.06.004

Koenigs, M., & Grafman, J. (2009). The functional neuroanatomy of depression: Distinct roles for ventromedial and dorsolateral prefrontal cortex. *Behavioural Brain Research*, *201*(2), 239–243. https://doi.org/10.1016/j.bbr.2009.03.004

Lakatos, M., Baranyi, M., Eross, L., Nardai, S., Torok, T. L., Sperlagh, B., & Vizi, E. S. (2020). Roles played by the Na^+/Ca^{2+} exchanger and hypothermia in the prevention of ischemia-induced carrier-mediated efflux of catecholamines into the extracellular space: Implications for stroke therapy. *Neurochemical Research*, *45*(1), 16–33. https://doi.org/10.1007/s11064-019-02842-0

Li, Y., Simmler, L. D., Van Zessen, R., Flakowski, J., Wan, J. X., Deng, F., Li, Y. L., Nautiyal, K. M., Pascoli, V., & Luscher, C. (2021). Synaptic mechanism underlying serotonin modulation of transition to cocaine addiction. *Science*, *373*(6560), 1252–1256. https://doi.org/10.1126/science.abi9086

Lilley, E., Stanford, S. C., Kendall, D. E., Alexander, S. P., Cirino, G., Docherty, J. R., … Ahluwalia, A. (2020). ARRIVE 2.0 and the *British Journal of Pharmacology*: Updated guidance for 2020. *British Journal of Pharmacology*, *177*(16), 3611–3616. Portico. https://doi.org/10.1111/bph.15178

Margolis, R. L. (2014). Tetrabenazine, depression and suicide: Good news. *Journal of Huntington's Disease*, *3*(2), 137–138. https://doi.org/10.3233/JHD-140107

Mathur, B. N., & Lovinger, D. M. (2012). Serotonergic action on dorsal striatal function. *Parkinsonism & Related Disorders*, *18*, S129–S131. https://doi.org/10.1016/s1353-8020(11)70040-2

Metzger, R. R., Brown, J. M., Sandoval, V., Rau, K. S., Elwan, M. A., Miller, G. W., Hanson, G. R., & Fleckenstein, A. E. (2002). Inhibitory effect of reserpine on dopamine transporter function. *European Journal of Pharmacology*, *456*(1–3), 39–43. https://doi.org/10.1016/s0014-2999(02)02647-x

Meyer, A. C., Horton, D. B., Neugebauer, N. M., Wooters, T. E., Nickell, J. R., Dwoskin, L. P., & Bardo, M. T. (2011). Tetrabenazine inhibition of monoamine uptake and methamphetamine behavioral effects: Locomotor activity, drug discrimination and self-administration. *Neuropharmacology*, *61*(4), 849–856. https://doi.org/10.1016/j.neuropharm.2011.05.033

Miller, D. K., Crooks, P. A., Zheng, G., Grinevich, V. P., Norrholm, S. D., & Dwoskin, L. P. (2004). Lobeline analogs with enhanced affinity and selectivity for plasmalemma and vesicular monoamine transporters. *The Journal of Pharmacology and Experimental Therapeutics*, *310*(3), 1035–1045. https://doi.org/10.1124/jpet.104.068098

Moll, G. H., Mehnert, C., Wicker, M., Bock, N., Rothenberger, A., Ruther, E., & Huether, G. (2000). Age-associated changes in the densities of presynaptic monoamine transporters in different regions of the rat brain from early juvenile life to late adulthood. *Brain Research. Developmental Brain Research*, *119*(2), 251–257. https://doi.org/10.1016/s0165-3806(99)00182-0

Morón, J. A., Brockington, A., Wise, R. A., Rocha, B. A., & Hope, B. T. (2002). Dopamine uptake through the norepinephrine transporter in brain regions with low levels of the dopamine transporter: Evidence from knock-out mouse lines. *Journal of Neuroscience*, *22*(2), 389–395. https://doi.org/10.1523/Jneurosci.22-02-00389.2002

Nickell, J. R., Siripurapu, K. B., Vartak, A., Crooks, P. A., & Dwoskin, L. P. (2014). The vesicular monoamine transporter-2: An important pharmacological target for the discovery of novel therapeutics to treat methamphetamine abuse. *Advances in Pharmacology*, *69*, 71–106. https://doi.org/10.1016/B978-0-12-420118-7.00002-0

Pearson, S. J., & Reynolds, G. P. (1988). Depletion of monoamine transmitters by tetrabenazine in brain tissue in Huntington's disease. *Neuropharmacology*, *27*(7), 717–719. https://doi.org/10.1016/0028-3908(88)90080-9

Percie du Sert, N., Ahluwalia, A., Alam, S., Avey, M. T., Baker, M., Browne, W. J., Clark, A., Cuthill, I. C., Dirnagl, U., Emerson, M., Garner, P., Holgate, S. T., Howells, D. W., Hurst, V., Karp, N. A., Lazic, S. E., Lidster, K., MacCallum, C. J., Macleod, M., … Wurbel, H. (2020). Reporting animal research: Explanation and elaboration for the ARRIVE guidelines 2.0. *PLoS Biology*, *18*(7), e3000411. https://doi.org/10.1371/journal.pbio.3000411

Raiteri, M., Angelini, F., & Levi, G. (1974). A simple apparatus for studying the release of neurotransmitters from synaptosomes. *European Journal of Pharmacology*, *25*(3), 411–414. https://doi.org/10.1016/0014-2999(74)90272-6

Ricciardi, L., Pringsheim, T., Barnes, T. R. E., Martino, D., Gardner, D., Remington, G., Addington, D., Morgante, F., Poole, N., Carson, A., & Edwards, M. (2019). Treatment recommendations for tardive dyskinesia. *Canadian Journal of Psychiatry*, *64*(6), 388–399. https://doi.org/10.1177/0706743719828968

Rice, M. E., & Cragg, S. J. (2008). Dopamine spillover after quantal release: Rethinking dopamine transmission in the nigrostriatal pathway. *Brain Research Reviews*, *58*(2), 303–313. https://doi.org/10.1016/j.brainresrev.2008.02.004

Robertson, S. D., Matthies, H. J., & Galli, A. (2009). A closer look at amphetamine-induced reverse transport and trafficking of the dopamine and norepinephrine transporters. *Molecular Neurobiology*, *39*(2), 73–80. https://doi.org/10.1007/s12035-009-8053-4

Roman, V., Kedves, R., Kelemen, K., Nemethy, Z., Sperlagh, B., Lendvai, B., & Vizi, E. S. (2021). Contribution of analog signaling to neurotransmitter interactions and behavior: Role of transporter-mediated nonquantal dopamine release. *Physiological Reports*, *9*(21), e15088. https://doi.org/10.14814/phy2.15088

Ross, S. B., & Renyi, A. L. (1966). In vitro inhibition of noradrenaline-3H uptake by reserpine and tetrabenazine in mouse cerebral cortex

tissues. *Acta Pharmacologica et Toxicologica (Copenh)*, *24*(1), 73–88. https://doi.org/10.1111/j.1600-0773.1966.tb00370.x

Santha, E., Sperlagh, B., Zelles, T., Zsilla, G., Toth, P. T., Lendvai, B., Baranyi, M., & Vizi, E. S. (2000). Multiple cellular mechanisms mediate the effect of lobeline on the release of norepinephrine. *The Journal of Pharmacology and Experimental Therapeutics*, *294*(1), 302–307. Retrieved from https://www.ncbi.nlm.nih.gov/pubmed/10871326

Schwarz, L. A., & Luo, L. (2015). Organization of the locus coeruleus-norepinephrine system. *Current Biology*, *25*(21), R1051–R1056. https://doi.org/10.1016/j.cub.2015.09.039

Spokes, E. G. (1980). Neurochemical alterations in Huntington's chorea: A study of post-mortem brain tissue. *Brain*, *103*(1), 179–210. https://doi.org/10.1093/brain/103.1.179

Steinbusch, H. W. (1981). Distribution of serotonin-immunoreactivity in the central nervous system of the rat-cell bodies and terminals. *Neuroscience*, *6*(4), 557–618. https://doi.org/10.1016/0306-4522(81)90146-9

Sudhof, T. C. (2012). The presynaptic active zone. *Neuron*, *75*(1), 11–25. https://doi.org/10.1016/j.neuron.2012.06.012

Vizi, E. S., Harsing, L. G. Jr., Zimanvi, I., & Gaal, G. (1985). Release and turnover of noradrenaline in isolated median eminence: Lack of negative feedback modulation. *Neuroscience*, *16*(4), 907–916. https://doi.org/10.1016/0306-4522(85)90105-8

Vizi, E. S., Ono, K., Adam-Vizi, V., Duncalf, D., & Foldes, F. F. (1984). Presynaptic inhibitory effect of Met-enkephalin on [^{14}C] acetylcholine release from the myenteric plexus and its interaction with muscarinic negative feedback inhibition. *The Journal of Pharmacology and Experimental Therapeutics*, *230*(2), 493–499. Retrieved from https://www.ncbi.nlm.nih.gov/pubmed/6747844

Vizi, E. S., Somogyi, G. T., Nagashima, H., Duncalf, D., Chaudhry, I. A., Kobayashi, O., Goldiner, P. L., & Foldes, F. F. (1987). Tubocurarine and pancuronium inhibit evoked release of acetylcholine from the mouse hemidiaphragm preparation. *British Journal of Anaesthesia*, *59*(2), 226–231. https://doi.org/10.1093/bja/59.2.226

Vizi, E. S., Zsilla, G., Caron, M. G., & Kiss, J. P. (2004). Uptake and release of norepinephrine by serotonergic terminals in norepinephrine transporter knock-out mice: Implications for the action of selective serotonin reuptake inhibitors. *The Journal of Neuroscience*, *24*(36), 7888–7894. https://doi.org/10.1523/JNEUROSCI.1506-04.2004

Volz, T. J., Hanson, G. R., & Fleckenstein, A. E. (2006). Kinetic analysis of developmental changes in vesicular monoamine transporter-2 function. *Synapse*, *60*(6), 474–477. https://doi.org/10.1002/syn.20321

Wang, H., Chen, X., Li, Y., Tang, T. S., & Bezprozvanny, I. (2010). Tetrabenazine is neuroprotective in Huntington's disease mice. *Molecular Neurodegeneration*, *5*, 18. https://doi.org/10.1186/1750-1326-5-18

Williams, G. V., & Goldman-Rakic, P. S. (1995). Modulation of memory fields by dopamine D1 receptors in prefrontal cortex. *Nature*, *376*(6541), 572–575. https://doi.org/10.1038/376572a0

Zsilla, G., Hegyi, D. E., Baranyi, M., & Vizi, E. S. (2018). 3,4-Methylenedioxymethamphetamine, mephedrone, and beta-phenylethylamine release dopamine from the cytoplasm by means of transporters and keep the concentration high and constant by blocking reuptake. *European Journal of Pharmacology*, *837*, 72–80. https://doi.org/10.1016/j.ejphar.2018.08.037

How to cite this article: Tod, P., Varga, A., Román, V., Lendvai, B., Pálkovács, R., Sperlágh, B., & Vizi, E. S. (2024). Tetrabenazine, a vesicular monoamine transporter 2 inhibitor, inhibits vesicular storage capacity and release of monoamine transmitters in mouse brain tissue. *British Journal of Pharmacology*, 1–16. https://doi.org/10.1111/bph.17348